Available online at www.sciencedirect.com
ScienceDirect
Catalysis Today 120 (2007) 292–297
CATALYSIS TODAY
www.elsevier.com/locate/cattod

Thermal decomposition of Li_3AlH_6 with $TiAl_3$ catalyst

Jae-Hyeok Shim [a], Gil-Jae Lee [a], Byeong-Joo Lee [b], Young-Joo Oh [a], Young Whan Cho [a,*]

[a] *Materials Science and Technology Division, Korea Institute of Science and Technology, Seoul 136-791, Republic of Korea*
[b] *Department of Materials Science and Engineering, Pohang University of Science and Technology, Pohang, Gyungbuk 790-784, Republic of Korea*

Available online 1 November 2006

Abstract

It has been found that the reaction products between $TiCl_3$ and Li_3AlH_6 by mechanical milling consist of LiCl and $TiAl_3$ together with TiH_2. Thermodynamic calculation also predicts that $TiAl_3$ becomes dominant over TiH_2 with increasing temperature. Based on this, ultra-fine $TiAl_3$ powder having the primary particle size of about 100 nm has been mechanochemically synthesized from a mixture of $TiCl_3$, $AlCl_3$ and Mg. The addition of this $TiAl_3$ powder into Li_3AlH_6 clearly shows a good catalytic effect on the thermal decomposition of Li_3AlH_6 as expected. The use of fine $TiAl_3$ catalyst is certainly more favorable than $TiCl_3$ in terms of hydrogen storage capacity as it does not produce irreversible chloride byproduct in alanates.

Keywords: Hydrogen storage materials; Alanate; Catalyst; Thermal decomposition; Mechanochemical synthesis

1. Introduction

The development of solid-state hydrogen storage at low and medium temperatures has been recognized as one of the key technologies for hydrogen fuel cell applications. Especially for vehicular applications, it is important to find new light-weight hydrogen storage materials that exhibit high reversible hydrogen capacity [1].

Alkali and alkali-earth metal alanates (aluminum hydrides) have received great attention as promising hydrogen storage materials owing to their inherent high theoretical hydrogen capacity, since Bogdanović and Schwickardi [2] first demonstrated in 1997 that reversible hydrogen storage could be achieved under moderate conditions (temperature and pressure) with accelerated kinetics in $NaAlH_4$ and Na_3AlH_6 by adding a small amount of Ti-containing catalysts such as $TiCl_3$ and $Ti(OBu)_4$ through wet chemistry. Following this finding, Jensen and his coworkers [3,4] reported improved kinetics by dispersing Ti-containing catalysts using a dry milling process. Currently, mechanical ball milling is being widely adopted to disperse a small amount of catalysts effectively into sodium alanates in solid state [5,6]. In addition to sodium alanates, it has been shown that other alanates such as lithium alanates could also be catalyzed with Ti-containing materials [7]. In spite of the outstanding performance of Ti-containing catalysts, there is still no clear understanding on how they play a catalytic role in alanates. The first step toward the understanding of this catalytic mechanism would be to confirm what form of Ti exists in alanates. However, it is quite difficult to confirm unambiguously the state of Ti (e.g. metallic Ti, Ti compounds or Ti substitution in alanates) in alanates using most analytical techniques, because a very small amount of Ti-containing catalysts are usually added. On the whole, there exit two hypotheses on the Ti state in alanates. While the results of recent investigations [8–12] seem to support the hypothesis that Ti in situ forms $TiAl_3$ when introduced into alanates, there is another hypothesis that Ti substitutes for metal sites in alanates [13–15].

Assuming that Ti does transform into $TiAl_3$ in alanates, it is worthwhile to confirm its efficacy by adding $TiAl_3$, instead of $TiCl_3$, into alanates because $TiCl_3$ permanently reduces hydrogen storage capacity of alanates by reacting with part of alanates to form very stable salts such as NaCl and LiCl. In fact, Balema et al. [8] and Resan et al. [16] have recently attempted to confirm the catalytic activity of $TiAl_3$ by dispersing $TiAl_3$ powder prepared by milling the arc melted

* Corresponding author. Tel.: +82 2 958 5465; fax: +82 2 958 5379.
E-mail address: oze@kist.re.kr (Y.W. Cho).

0920-5861/$ – see front matter
doi:10.1016/j.cattod.2006.09.005

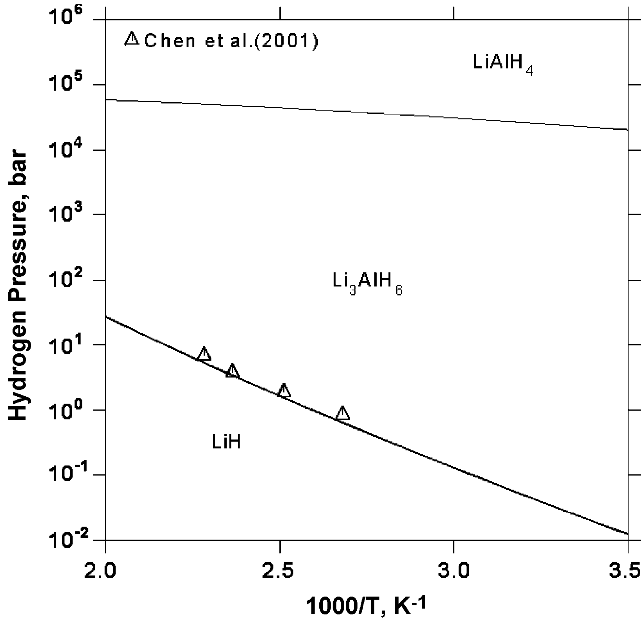

Fig. 1. Calculated stability diagram of LiH, Li_3AlH_6 and $LiAlH_4$ [18].

sample and commercial powder (<150 μm), respectively, into $LiAlH_4$. They showed that the addition of $TiAl_3$ indeed decreased the dehydrogenation starting temperature of $LiAlH_4$ by about 10 °C, although the catalytic effect may not be significant. It is, therefore, desirable to produce as fine $TiAl_3$ powder as possible as the catalytic efficacy will be naturally enhanced with decreasing particle size of catalyst. Mechanical milling is one of the simple and cost-effective methods for producing $TiAl_3$ powders. However, it might be difficult to obtain fine $TiAl_3$ particles using conventional milling techniques because $TiAl_3$ is relatively ductile and thus they easily agglomerate during milling [17].

The purpose of this study is to elucidate if $TiCl_3$ indeed forms $TiAl_3$ in Li_3AlH_6 using both experimental work and theoretical calculations and to investigate the catalytic effect of $TiAl_3$ on thermal decomposition (dehydrogenation) of Li_3AlH_6 using ultrafine $TiAl_3$ powder prepared by mechanochemical reaction between $TiCl_3$, $AlCl_3$ and Mg powders. The main reason to adopt Li_3AlH_6 (5.6 wt.% H_2) instead of $LiAlH_4$ (7.9 wt.% H_2) is that the hydrogen pressure required to re-hydrogenate $LiAlH_4$ is estimated to be an order of 10^4 bar, according to our recent thermodynamic calculation shown in Fig. 1 [18].

2. Experimental procedure

$LiAlH_4$ (95%), LiH (95%), $TiCl_3$ (99%) and $AlCl_3$ (99.9%) powders were purchased from Sigma–Aldrich, and Mg (99.8%) powder from Alfa–Aesar. In order to synthesize Li_3AlH_6 mechanochemically, a 5 g mixture of $LiAlH_4$ and LiH with a molar ratio of 1:2 was charged together with ten 15 mm and thirty 10 mm diameter zirconia balls into a 250 ml silicon nitride bowl under an argon atmosphere in a glove box. The ball-to-powder weight ratio was approximately 37:1. The mixture was milled in a Fritsch P4 planetary mill at 350 rpm for 4 h 30 min.

A 1 g mixture of mechanochemically prepared Li_3AlH_6 and $TiCl_3$ was charged together with seventeen 7.9 mm diameter Cr-steel balls into a tool steel vial under an argon atmosphere. The ball-to-powder weight ratio was approximately 35:1. The mixture was milled in a SPEX-8000 mill for 2 h. Some of the milled powders were rinsed in distilled water and filtered to remove chloride formed during milling. The mole ratio between Li_3AlH_6 and $TiCl_3$ was changed from 1:1 to 6:1.

In order to synthesize fine $TiAl_3$ mechanochemically, a mixture of $TiCl_3$, $AlCl_3$ and Mg powders with a molar ratio of 1:3:6 was milled for 4 h using the SPEX-8000 mill at the same milling condition as described before. The milled powder was rinsed in distilled water and filtered to remove $MgCl_2$ byproduct formed during milling.

The product powders were characterized by X-ray diffraction (XRD) using Bruker D8 Advance with Cu Kα radiation and scanning electron microscopy (SEM) using FEI XL-30 FEG.

In order to confirm the catalytic effect of fine $TiAl_3$ on the thermal decomposition of Li_3AlH_6, 5 mol% $TiAl_3$ was dispersed into Li_3AlH_6 by milling the mixture in the SPEX-8000 mill for 30 min. The same amount of $TiCl_3$ was also dispersed into Li_3AlH_6 for comparison. The thermal decomposition behavior of Li_3AlH_6 with and without catalyst was analyzed by differential scanning calorimetry (DSC) using NETSCH DSC204 and thermogravimetry (TG) using NETSCH TG209. The heating rate was 2 °C/min and the flow rate of 99.9999% argon gas was 50 ml/min for both DSC and TG measurements. The kinetics of the thermal decomposition reaction was volumetrically measured by a Sievert type apparatus.

3. Thermodynamic calculation

Thermodynamic calculation of the Li–Al–H–Ti–Cl system was performed based on the Gibbs-energy minimization criterion [19] to understand what the equilibrium phases are in the Li_3AlH_6 and $TiCl_3$ mixtures. The phases included in this calculation were Li_3AlH_6, $LiAlH_4$, LiH, $TiCl_3$, LiCl, Ti, Al, TiAl, $TiAl_3$, Ti_3Al, $TiAl_2$, Ti_5Al_{11}, TiH_2 and H_2. The Gibbs energy data for Li_3AlH_6 and $LiAlH_4$ were taken from Ref. [18]. The data for the Ti–Al intermetallic phases and all the other phases were from the SGTE solution and substance databases, respectively, which are incorporated into Thermo-Calc [20].

4. Results and discussion

The XRD pattern of the mixture of $LiAlH_4$ and LiH milled for 4 h 30 min is presented in Fig. 2. The peak positions are in good agreement with those of Li_3AlH_6 obtained by Zaluski et al. [21] and Balema et al. [22]. It is, therefore, confirmed that Li_3AlH_6 forms during milling according to the following reaction:

$$LiAlH_4 + 2LiH \rightarrow Li_3AlH_6 \quad (1)$$

The XRD patterns of reaction products between $LiAlH_6$ and $TiCl_3$ milled for 2 h are shown in Fig. 3. For the 6:1 mixture,

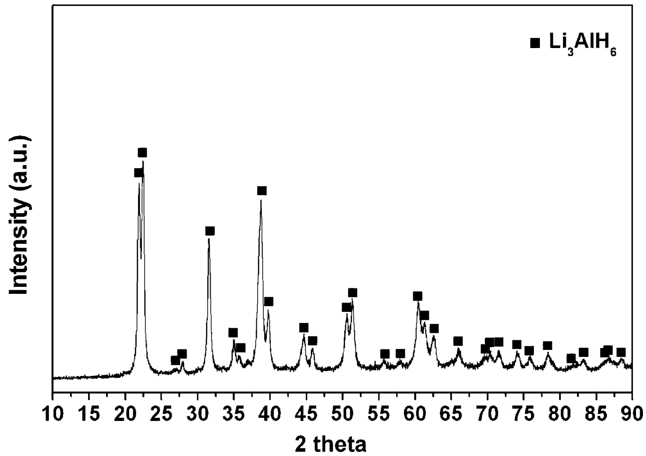

Fig. 2. XRD pattern of Li_3AlH_6 prepared by mechanochemical reaction.

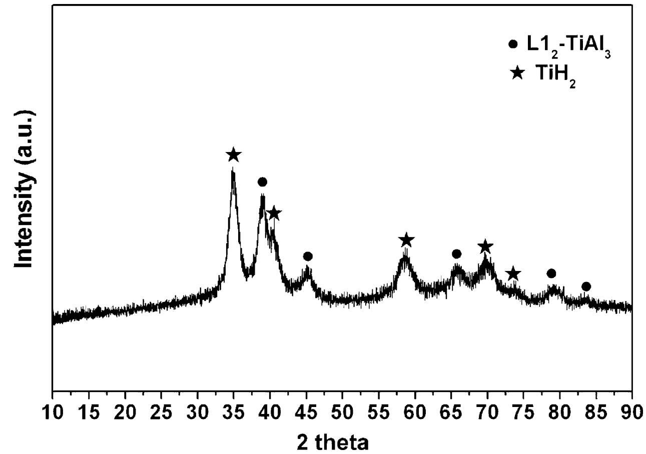

Fig. 4. XRD pattern of reaction products between Li_3AlH_6 and $TiCl_3$ (1:1 mixture) after rinsing in distilled water.

LiCl and $TiAl_3$ with $L1_2$ structure form and very small peaks of Li_3AlH_6 are also observed in the pattern. In the cases of the 2:1 and 1:1 mixtures, Li_3AlH_6 disappears, while LiCl and $L1_2$–$TiAl_3$ are still the main products. It is found, however, that there exists another reaction product in the 1:1 mixture (Fig. 3c). This phase could be indexed as δ-TiH_2 with cubic structure, although the strongest peak of it overlaps those of LiCl and $TiAl_3$. The reaction product of the 1:1 mixture was rinsed in distilled water after milling in order to make the phase identification easy by removing LiCl. The XRD pattern of the rinsed reaction products is given in Fig. 4. The presence of δ-TiH_2 is clearly shown together with $L1_2$–$TiAl_3$. From these mechanochemical reactions with various mixing ratios between Li_3AlH_6 and $TiCl_3$, it is concluded that $TiCl_3$ transforms mainly into $L1_2$–$TiAl_3$ when it is introduced in Li_3AlH_6 as catalyst and starts to produce δ-TiH_2 at high concentrations of $TiCl_3$. The formation of $L1_2$–$TiAl_3$ was also observed when a 3:1 mixture of $NaAlH_4$ and $TiCl_3$ was ball milled [9].

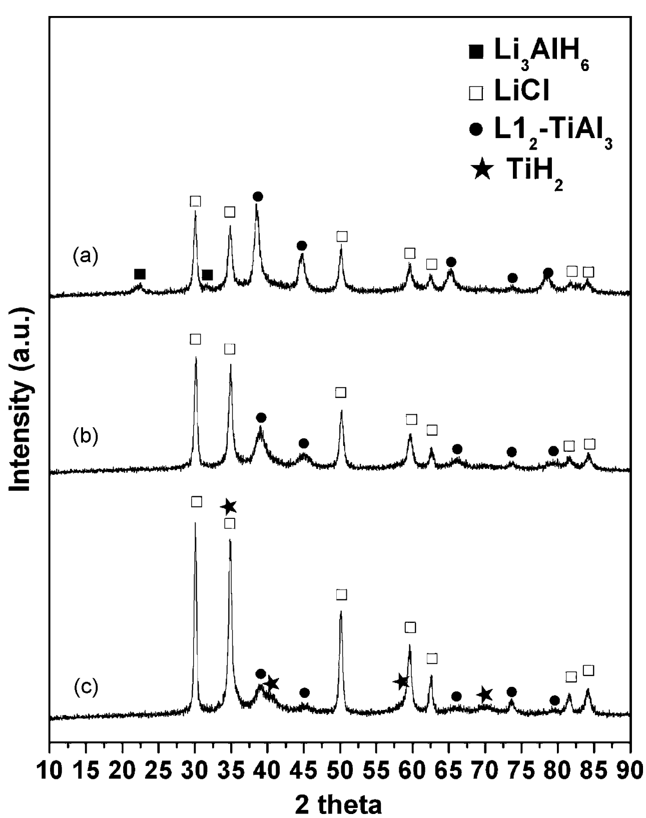

Fig. 3. XRD patterns of reaction products between Li_3AlH_6 and $TiCl_3$: (a) 6:1, (b) 2:1, and (c) 1:1.

The formation of $L1_2$–$TiAl_3$ in alanates with $TiCl_3$ catalyst during milling is quite interesting, because the equilibrium phase at 75 at.% Al in the Ti–Al phase diagram is not cubic $L1_2$- but tetragonal $D0_{22}$-$TiAl_3$. Although $D0_{22}$-$TiAl_3$ is energetically more stable than $L1_2$ by about 0.05 eV/atom [23], $L1_2$–$TiAl_3$ rather than $D0_{22}$ is frequently observed when the process conditions are far from equilibrium such as mechanical milling and thin film deposition [24]. The formation of metastable $L1_2$–$TiAl_3$ might be attributed to its lower kinetic nucleation barrier compared to equilibrium $D0_{22}$-$TiAl_3$, because the $L1_2$ structure shows a lower degree of order than $D0_{22}$ [24]. Moreover, it has been known for a long time that the third elements such as Cu, Cr, Fe, Ni and Mn stabilize the $L1_2$ structure [25]. Impurity elements such as Fe, which might have been introduced by erosion from balls and vials during milling, probably helped stabilize $L1_2$–$TiAl_3$.

Table 1 summarizes the result of the thermodynamic calculation for the reaction products between Li_3AlH_6 and $TiCl_3$ at 25 °C. In this calculation, $D0_{22}$-$TiAl_3$ instead of $L1_2$–$TiAl_3$ was taken into account because thermodynamic data of $L1_2$–$TiAl_3$ is not available. Thermodynamics tells that

Table 1
Calculated equilibrium phase fractions at 25 °C

Mixing ratios of Li_3AlH_6 and $TiCl_3$		
6:1	2:1	1:1
Phase fraction (%)		
H_2 7.3	H_2 19.4	H_2 33.3
LiCl 9.3	LiCl 25.0	LiCl 42.9
$TiAl_3$ 2.1	$TiAl_3$ 5.6	$TiAl_3$ 9.5
TiH_2 3.1	TiH_2 8.3	TiH_2 14.3
Li_3AlH_6 78.1	Li_3AlH_6 41.7	Li_3AlH_6 0.0

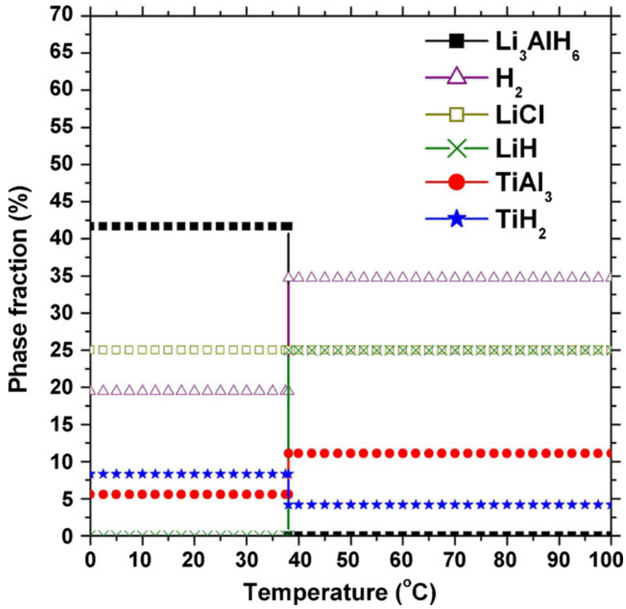

Fig. 5. Calculated equilibrium phase fractions in 2:1 mixture of Li_3AlH_6 and $TiCl_3$ between 0 and 100 °C.

LiCl and $TiAl_3$ are the equilibrium reaction products, which is in good agreement with the results of the present milling experiments. However, TiH_2 always appears along with $TiAl_3$, which shows only partial agreement with the experiment. TiH_2 is observed only in the 1:1 mixture. In addition, Li_3AlH_6 is not observed in the experiment although it remains as a stable phase in the 2:1 mixture according to the calculation. The calculated mole fractions of the equilibrium phases for the 2:1 mixture between 0 and 100 °C are shown in Fig. 5. Interestingly, the mole fraction of $TiAl_3$ increases and that of TiH_2 decreases with increasing temperature. $TiAl_3$ becomes dominant over TiH_2 and Li_3AlH_6 disappears as the mole fraction of $TiAl_3$ increases above about 40 °C. This is probably because TiH_2 reacts with Li_3AlH_6 to form $TiAl_3$. The temperature inside the vial, surely, increases by the collisions between balls and vial walls during milling, although it is difficult to measure or predict the exact temperature increase. The increase in temperature during milling might explain why TiH_2 and Li_3AlH_6 are not clearly observed in the 6:1 and 2:1 mixtures. It is shown in Fig. 5 that LiH forms by the decomposition of Li_3AlH_6. By chance, the peaks of LiH are almost coincident with $L1_2$–$TiAl_3$ in the XRD pattern. The overlap of the peaks seems to make the peaks of $TiAl_3$ relatively high in the XRD patterns of the 6:1 and 2:1 mixtures compared to those of the 1:1 mixture, as shown in Fig. 3a and b.

The XRD patterns of the mixture of $TiCl_3$, $AlCl_3$ and Mg milled for 4 h and the sample rinsed in distilled water after milling are presented in Fig. 6. $L1_2$–$TiAl_3$ and $MgCl_2$ are identified as the main reaction products after milling (Fig. 6a) and the starting materials such as $TiCl_3$, $AlCl_3$ and Mg are not observed. This indicates that the following reaction is completed after 4 h of milling:

$$TiCl_3 + 3AlCl_3 + 6Mg \rightarrow TiAl_3 + 6MgCl_2 \quad (2)$$

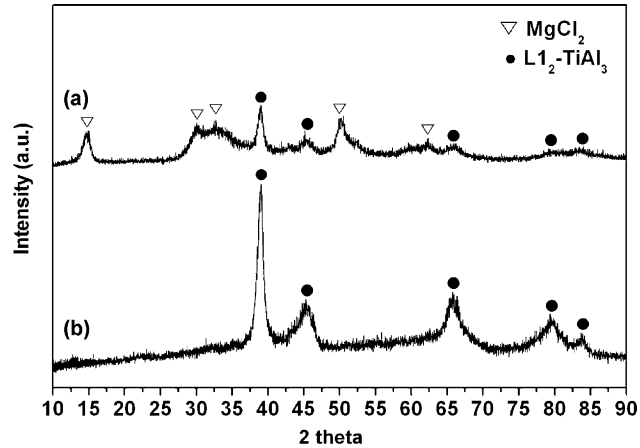

Fig. 6. XRD patterns of the $TiCl_3$, $AlCl_3$ and Mg mixture (b) milled for 4 h and (a) rinsed in distilled water after the milling.

As shown in Fig. 6b, relatively pure $TiAl_3$ is easily obtained as $MgCl_2$ formed during milling is completely dissolved in distilled water and washed away during filtering.

Fig. 7 shows an SEM micrograph of the $TiAl_3$ powder. The primary particle size is around 100 nm and it exhibits an irregular shape, although most particles seem to be agglomerated. Compared to coarse particle size (>10 μm) of $TiAl_3$ obtained from milling of a mixture of Ti and Al powders, they are extremely fine. It can be concluded that this chloride-based mechanochemcal reaction is very effective in reducing the size of product particle, as Tsuzuki and McCormick [26] showed for various reaction systems.

The XRD patterns of Li_3AlH_6 catalyzed with $TiAl_3$ and $TiCl_3$ are presented in Fig. 8. Although most of $TiAl_3$ peaks except for (2 2 0) overlap with those of Li_3AlH_6, it seems that $TiAl_3$ is stable in Li_3AlH_6 without any reaction or transformation (Fig. 8a). In the case of Li_3AlH_6 catalyzed with $TiCl_3$, the formation of LiCl is clearly shown in the XRD pattern (Fig. 8b), although the existence of $TiAl_3$ is not so evident with a small amount of $TiCl_3$. This is presumably because the crystallite size of $TiAl_3$ in situ formed in Li_3AlH_6 is too small to identify with XRD. In fact, Graetz et al. [10] reported that the formation of nanocrystalline $TiAl_3$ in $NaAlH_4$ catalyzed with 2 and 4 mol% $TiCl_3$ was observed by high-energy X-ray absorption.

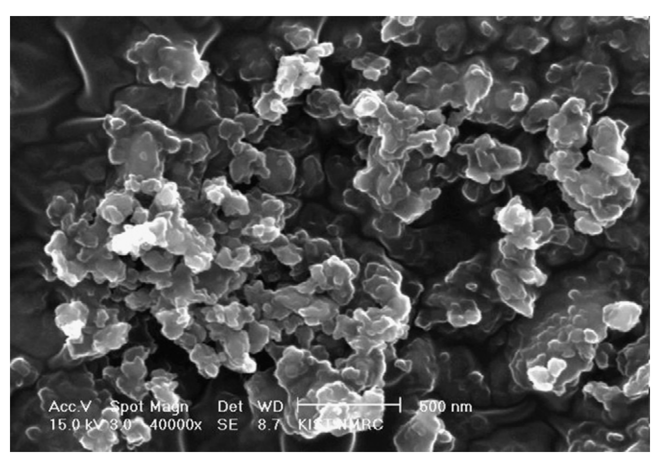

Fig. 7. SEM micrograph of the synthesized $TiAl_3$ powder.

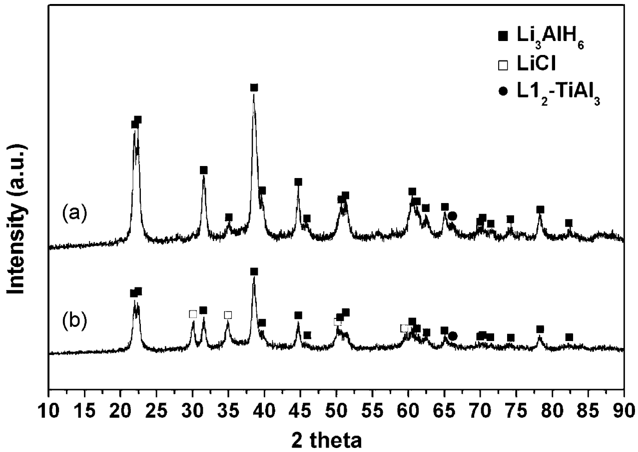

Fig. 8. XRD patterns of Li_3AlH_6 catalyzed with (a) $TiAl_3$ and (b) $TiCl_3$.

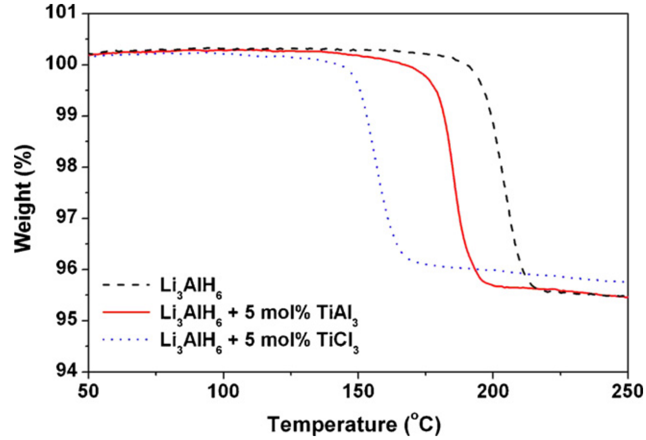

Fig. 10. TG curves of Li_3AlH_6 with and without catalysts.

Fig. 9 shows DSC curves of Li_3AlH_6 with and without catalysts. All the samples exhibit a large endothermic peak according to the following thermal decomposition reaction:

$$Li_3AlH_6 \rightarrow 3LiH + Al + \frac{3}{2}H_2 \tag{3}$$

Without catalysts, Li_3AlH_6 starts to decompose releasing H_2 gas (dehydrogenation) at about 190 °C and the peak temperature is about 210 °C. On the other hand, the thermal decomposition of Li_3AlH_6 containing $TiAl_3$ starts at about 160 °C and exhibits the peak at about 180 °C. This decrease in thermal decomposition temperature is quite large compared to those of Balema et al. [8] and Resan et al. [16] who had also used $TiAl_3$. This might be attributed to the ultrafine particle size of $TiAl_3$ prepared in the present work. Nevertheless, the catalytic efficacy of ultrafine $TiAl_3$ is not as good as that of $TiCl_3$, which decreases the thermal decomposition starting temperature down to about 130 °C. It is not fully understood yet why there exists a difference in catalytic activity between externally added and in situ formed $TiAl_3$ particles. This is presumably because the in situ formation and dispersion of $TiAl_3$ by the reaction between $TiCl_3$ and Li_3AlH_6 is more advantageous than the direct dispersion of $TiAl_3$ in aspects of the uniform dispersion and fine particle size of the catalyst. Oxide layers inevitably exist on the surface of the externally added $TiAl_3$ particles, which had formed during the rinsing and filtering processes, might have decreased the catalytic activity.

The TG curves show the amount of released hydrogen as well as the thermal decomposition temperature (Fig. 10). Li_3AlH_6 without catalysts releases about 4.8 wt.% H_2, which is lower than the theoretical hydrogen storage capacity of Li_3AlH_6 (5.6 wt.%) due to the low purity of raw materials and the partial decomposition of Li_3AlH_6 during mechanochemical preparation. It is noted that Li_3AlH_6 catalyzed with $TiAl_3$ releases larger amount of hydrogen (4.5 wt.%) than Li_3AlH_6 with $TiCl_3$ (4.0 wt.%) as expected. This is evident because $TiCl_3$ decomposes part of Li_3AlH_6 during milling for dispersion and thus decreases the hydrogen storage capacity of Li_3AlH_6. Therefore, it will be favorable to add $TiAl_3$ instead of $TiCl_3$ into alanates in order to minimize the loss in hydrogen storage capacity of Li_3AlH_6.

The thermal decomposition kinetics of Li_3AlH_6 with and without catalysts at 150 °C is shown in Fig. 11. Without catalysts, Li_3AlH_6 shows slow thermal decomposition kinetics,

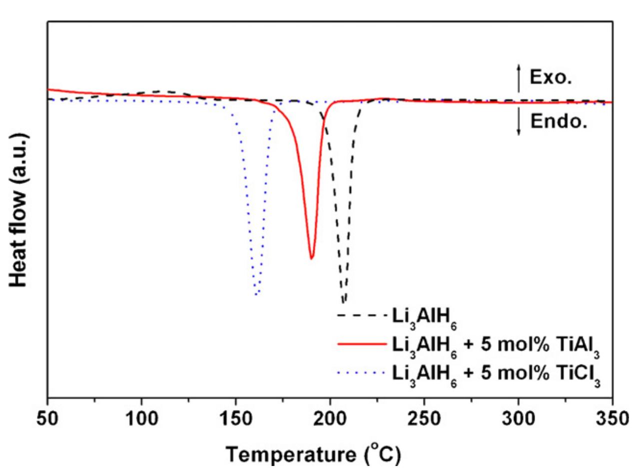

Fig. 9. DSC curves of Li_3AlH_6 with and without catalysts.

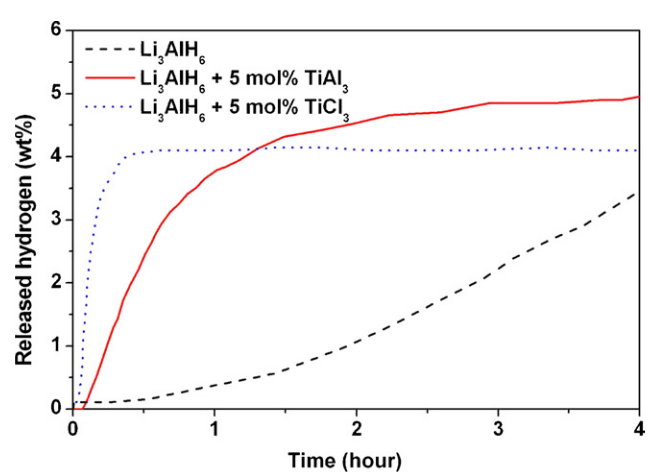

Fig. 11. Amount of hydrogen released from Li_3AlH_6 during thermal decomposition at 150 °C as a function of time.

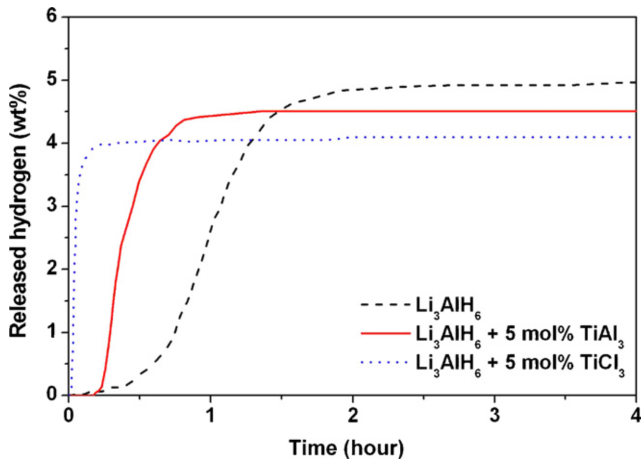

Fig. 12. Amount of hydrogen released from Li_3AlH_6 during thermal decomposition as a function of time at 170 °C.

releasing at most about 3.4 wt.% hydrogen in 4 h. It is found that the addition of $TiAl_3$ significantly improves the thermal decomposition kinetics. The amount of hydrogen released from Li_3AlH_6 catalyzed with $TiAl_3$ exceeds that with $TiCl_3$ at 90 min and is saturated to about 4.5 wt.% in 3 h. Li_3AlH_6 catalyzed with $TiCl_3$ finally releases only about 4.0 wt.% hydrogen, although it shows the fastest kinetics. The $TiAl_3$ catalyst exhibits the improved kinetics, also at 170 °C, compared to Li_3AlH_6 without catalysts, releasing about 4.5 wt.% hydrogen in an hour (Fig. 12).

Despite the importance of Ti-containing catalysts in alanates, the catalytic mechanism in the dehydrogenation and re-hydrogenation reactions is still not fully understood, although there have been some attempts to explain the mechanisms [12,27]. In order to enhance the performance of known catalysts and to develop new catalysts, the exact mechanism should be further elucidated.

5. Conclusions

The present investigation shows that the reaction between $TiCl_3$ and Li_3AlH_6 by mechanical milling produces LiCl and $L1_2$–$TiAl_3$. δ-TiH_2 is also observed when the $TiCl_3$ concentration is high in the starting mixture. The formation of both $TiAl_3$ and TiH_2 is in good agreement with the result of thermodynamic calculation, though $TiAl_3$ becomes more favorable phase than TiH_2 as temperature increases. The addition of ultrafine $TiAl_3$ powder, synthesized by mechanochemical reaction between $TiAl_3$, $AlCl_3$ and Mg, into Li_3AlH_6 decreases the thermal decomposition temperature by about 30 K and significantly improved the decomposition reaction kinetics, compared to Li_3AlH_6 without any catalyst. Although this ultrafine $TiAl_3$ catalyst is still not as good as $TiCl_3$, particularly in terms of reaction kinetics, it is demonstrated in the present study that the use of $TiAl_3$ catalyst is more desirable than $TiCl_3$ in terms of hydrogen storage capacity.

Acknowledgements

This work has been supported by the Hydrogen Energy R&D Center, one of the 21st Century Frontier R&D Programs, funded by the Ministry of Science and Technology of Korea.

References

[1] L. Schlapbach, A. Züttel, Nature 414 (2001) 353.
[2] B. Bogdanović, M. Schwickardi, J. Alloys Compd. 253/254 (1997) 1.
[3] C.M. Jensen, R. Zidan, N. Mariels, A. Hee, C. Hagen, Int. J. Hydrogen Energy 24 (1999) 461.
[4] R.A. Zidan, S. Takara, A.G. Hee, C.M. Jensen, J. Alloys Compd. 285 (1999) 119.
[5] K.J. Gross, G.J. Thomas, C.M. Jensen, J. Alloys Compd. 330–332 (2002) 683.
[6] G. Sandrock, K. Gross, G. Thomas, J. Alloys Compd. 339 (2002) 299.
[7] J. Chen, N. Kuriyama, Q. Xu, H.T. Takeshita, T. Sakai, J. Phys. Chem. B 105 (2001) 11214.
[8] V.P. Balema, J.W. Wiench, K.W. Dennis, M. Pruski, V.K. Pecharsky, J. Alloys Compd. 329 (2001) 108.
[9] E.H. Majzoub, K.J. Gross, J. Alloys Compd. 356/357 (2003) 363.
[10] J. Graetz, J.J. Reilly, J. Johnson, A.Yu. Ignatov, T.A. Tyson, Appl. Phys. Lett. 85 (2004) 500.
[11] A.G. Haiduc, H.A. Stil, M.A. Schwarz, P. Paulus, J.J.C. Greerlings, J. Alloys Compd. 393 (2005) 252.
[12] V.P. Balema, L. Balema, Phys. Chem. Chem. Phys. 7 (2005) 1310.
[13] D. Sun, T. Kiyobayashi, H.T. Takeshita, N. Kuriyama, C.M. Jensen, J. Alloys Compd. 337 (2002) L8.
[14] J. Íñiguez, T. Yildirim, T.J. Udovic, M. Sulic, C.M. Jensen, Phys. Rev. B 70 (2004) 060101(R).
[15] O.M. Løvvik, S.M. Opalka, Phys. Rev. B 71 (2005) 054103.
[16] M. Resan, M.D. Hampton, J.K. Lomness, D.K. Slattery, Int. J. Hydrogen Energy 30 (2005) 1417.
[17] K.I. Moon, K.S. Lee, J. Alloys Compd. 264 (1998) 258.
[18] J.-W. Jang, J.-H. Shim, Y.W. Cho, B.-J. Lee, J Alloys Compd. 420 (2006) 286.
[19] N. Saunders, A.P. Miodownik, CALPHAD: A Comprehensive Guide, Elsevier Science, Oxford, UK, 1998.
[20] http://www.thermocalc.se.
[21] L. Zaluski, A. Zaluska, J.O. Ström-Olsen, J. Alloys Compd. 290 (1999) 71.
[22] V.P. Balema, V.K. Pecharsky, K.W. Dennis, J. Alloys Compd. 313 (2000) 69.
[23] T. Hong, T.J. Watson-Yang, A.J. Freeman, T. Oguchi, J. Xu, Phys. Rev. B 41 (1990) 12462.
[24] T. Klassen, M. Oehring, R. Bormann, J. Mater. Res. 9 (1994) 47.
[25] S.S. Nayak, B.S. Murty, Mater. Sci. Eng. A367 (2004) 218.
[26] T. Tsuzuki, P.G. McCormick, J. Mater. Sci. 39 (2004) 5143.
[27] http://www.eere.energy.gov/hydrogenandfuelcells/pdfs/annual04/iiic2_wang.pdf.